C Journal of Carbon Research

MDPI

Article

Selection of Mixed Amines in the CO_2 Capture Process

Pao-Chi Chen *, Hsun-Huang Cho, Jyun-Hong Jhuang and Cheng-Hao Ku

Department of Chemical and Materials Engineering, Lunghwa University of Science and Technology, Taoyuan 33306, Taiwan; doraemon31906@gmail.com (H.-H.C.); a0909562768@gmail.com (J.-H.J.); d1074142033@gm.lhu.edu.tw (C.-H.K.)

* Correspondence: chenpc@mail2000.com.tw

Abstract: In order to select the best mixed amines in the CO_2 capture process, the absorption of CO_2 in mixed amines was explored at the required concentrations by using monoethanolamine (*MEA*) as a basic solvent, mixed with diisopropanolamine (DIPA), triethanolamine (TEA), 2-amino-2-methyl-1-propanol (*AMP*), and piperazine (*PZ*). Here, a bubble column was used as the scrubber, and a continuous operation was adopted. The Taguchi method was used for the experimental design. The conditional factors included the type of mixed amine (A), the ratio of the mixed amines (B), the liquid feed flow (C), the gas-flow rate (D), and the concentration of mixed amines (E). There were four levels, respectively, and a total of 16 experiments. The absorption efficiency (E_F), absorption rate (R_A), overall mass transfer coefficient (K_Ga), and scrubbing factor (ϕ) were used as indicators and were determined in a steady-state by the mass balance and two-film models. According to the Taguchi analysis, the importance of the parameters and the optimum conditions were obtained. In terms of the absorption efficiency (E_F), the absorption rate (absorption factor) (R_A/ϕ), and the overall mass transfer coefficient (K_Ga), the order of importance is D > E > A > B > C, D > E > C > B > A, and D > E > C > A > B, respectively, and the optimum conditions are A1B4C4D3E3, A1B3C4D4E2, A4B2C3D4E4, and A1B1C1D4E1. The optimum condition validation results showed that the optimal values of E_F, R_A, and K_Ga are 100%, 30.69 $\times$ 10^{-4} mol/s·L, 1.540 l/s, and 0.269, respectively. With regard to the selection of mixed amine, it was found that the mixed amine (*MEA* + *AMP*) performed the best in the CO_2 capture process.

Keywords: amine; bubble-column scrubber; Taguchi method; overall mass transfer coefficient

Citation: Chen, P.-C.; Cho, H.-H.; Jhuang, J.-H.; Ku, C.-H. Selection of Mixed Amines in the CO_2 Capture Process. *C* **2021**, *7*, 25. https://doi.org/10.3390/c7010025

Received: 13 January 2021
Accepted: 19 February 2021
Published: 24 February 2021

1. Introduction

Currently, carbon dioxide (CO_2) emissions are a major issue worldwide, especially in industry, and coal-fired power plants are the most concerning source. To reduce CO_2 emissions, several studies on the capture, storage, and reuse of CO_2 have been explored. They have focused mainly on post-combustion and used the absorption method [1–3], which uses an alkaline solution to capture the CO_2. The absorption of CO_2 in an alkaline solution is also an effective method that is used for the removal of CO_2 from flue gas; it adopts a lot of solvents, including amines, amino salts, sodium hydroxide solution, and bicarbonate solutions [4]. To date, monoethanolamine (*MEA*) has been used as a wilder solvent to capture CO_2 and hydrogen sulfide, due to its lower cost and higher boiling point, compared to other solvents [5,6]. The important industrial alkanolamines are *MEA*, diethanolamine (*DEA*), aminomethyl propanol (TEA), and methyldiethanolamine (*MDEA*). However, 2-amino-2-methyl-1-propanol (*AMP*) and piperazine (*PZ*) [7–10] are always used as an absorption solvent and promoter, respectively. Here, amines can be divided into four classes, namely: primary amines (such as *MEA* and diglycolamine (DGA)), secondary amines (such as *DEA* and diisopropylamine (DIPA)), tertiary amines (such as TEA and *MDEA*), and steric hindrance amines (such as *AMP*). The properties and drawbacks of each class of amine are listed in Table 1. In addition, the loading of *MEA* is limited by stoichiometry to 0.5 moles CO_2 per mole amine. However, the loading is higher for

secondary and tertiary amines, which have higher loadings of up to 1 mole of CO_2 per mole of amine. The primary and secondary amines react rapidly with CO_2 to form carbamates, which results in higher solvent regeneration costs. On the other hand, tertiary amines catalyze the CO_2 hydrolysis reduction, forming bicarbonate ions and protonated amines. The heat of the reaction in bicarbonate formation is lower than that in carbamate formation, thus reducing the solvent regeneration costs. However, tertiary amines react more slowly with CO_2 than primary and secondary amines. In addition, *PZ*, which is a cyclic diamine, can be used as an activator [11,12].

Table 1. The properties and limitations of various amines.

Amine	Chemical Structure	Advantage	Drawback	References
Primary amine	H_2N-CH_2-CH_2-OH (*MEA*) H_2N-CH_2-CH_2-O-CH_2-CH_2-OH (DGA)	• High absorption rate • Cheaper • Lower viscosity	• Lower absorption capacity • Higher heat capacity • It cannot be used to absorb COS and CS_2 mixed gas • Higher vapor pressure • Higher heat regeneration cost	[12]
Secondary amine	HN-(CH_2-CH_2-OH)$_2$ (*DEA*) HN-(CH_2-C(OH)-CH_3)$_2$ (DIPA)	• It can be used to capture COS and CS_2 gases • Higher loading • Lower heat capacity • Lower vapor pressure • Cheaper • Lower heat of reaction • Less corrosive than *MEA*	• Higher viscosity • A limited solubility in water	[9]
Tertiary amine	N-(CH_2-CH_2-OH)$_3$ (TEA) CH_3-N-(CH_2-CH_2-OH)$_2$ (*MDEA*)	• Higher loading • Lower heat capacity • Lower vapor pressure • Lower heat of reaction	• Lower absorption rate • More expensive • Higher viscosity	[13,14]
Steric hindrance	HN-CH-(CH_3)$_2$-CH_2-OH (*AMP*)	• Higher loading • Higher absorption rate and higher loading • Good stripping property	• Higher heat capacity • More expensive • Higher viscosity	[15,16]
Piperazine	$C_4H_{10}N_2$ (*PZ*)	• Anti-oxidative • Anti-thermal degradation • Promote reaction rate	• Water and CO_2 absorption in air	[8]

The absorption of acid gases, by using mixed amines, has an advantage over the use of single amines [9,15,17]. Therefore, the rapidly-rising energy demands have led to the development of more efficient solvents for the absorption of CO_2 gas [11,14,18–24]. The absorption rate of CO_2 into the mixed amines of *MEA* + *MDEA* and *MEA* + TEA has been studied by several authors [13,25,26]. The use of *AMP* + *MEA* as an effective solvent was reported in the literature [15]. The mixed amine systems, which combine the higher equilibrium capacity of the tertiary amine (*MDEA*) with the higher reaction rate of the primary (*MEA*) and secondary amine (*DEA*), can bring about a considerable improvement in the gas absorption rate. The addition of piperazine to potassium carbonate, *MEA*, tertiary amine, and steric hindrance amine, to enhance the reaction rate, has been explored [16,19]. Most of these studies have reported the kinetics of the reaction of CO_2 with different amine blends [9,15–17,19].

In *MEA* aqueous solutions, two mechanisms for the formation of carbamate have been proposed: one is the zwitterions mechanism, and the other is the termolecular mechanism [6,27]. This termolecular mechanism assumes that an amine reacts simultaneously with one molecule of CO_2 and one molecule of a base, and forms an intermediate loosely-bound complex. The reaction between CO_2 and the amine can be described by a two-step

zwitterions mechanism [6,14]. The chemistry equations can be reduced to three important steps, i.e., carbamate formation, bicarbonate formation, and carbamate reversion:

Carbamate formation:

$$CO_2 + 2RNH_2 = RNHCOO^- + RNH_3^+ \quad (1)$$

Bicarbonate formation:

$$CO_2 + RNH_2 + H_2O = HCO_3^- + RNH_3^+ \quad (2)$$

Carbamate reversion:

$$RNHCOO^- + CO_2 + 2H_2O = 2RNH_3^+ + HCO_3^- \quad (3)$$

The total reaction rate of all CO_2 reactions in an aqueous solution is shown below:

$$r = k_{obs}(CO_2) \quad (4)$$

where, k_{obs} is the observed reaction rate constant, which is defined as follows:

$$k_{obs} = \left[\frac{k_1(RNH_2)}{1 + \frac{k_{-1}}{k_B(B)}}\right] + [k_{H_2O}(H_2O) + k_{OH^-}(OH^-)] \quad (5)$$

where k_1 is the forward reaction rate constant in Equation (1), k_{-1} is the backward reaction rate constant in Equation (1), k_B is the rate constant in Equation (2), and k_{OH^-} is the reaction constant of CO_2 with OH^-. The overall reaction rate depends on the concentration of hydroxyl ions, which increases with the pK_a value of the amine [6]. At a high concentration of RNH_2, the absorption rate of CO_2 is greater, but more $RNHCOO^-$ is produced and, hence, more bicarbonate, as shown in Equations (1) and (2). Therefore, the method of controlling the chemical species in the $CO_2/MEA/H_2O$ system is significant in the CO_2 capture process.

During the absorption of CO_2 with mixed amines, the reaction rate of the bicarbonate ion is very slow, and thus $r_{HCO_3^-}$ is neglected. Therefore, the kinetics of individual amine for the case of $k_{-1}/(\sum(k_b[B]) << 1$, which is second-order kinetics, can be expressed as follows [12]:

$$r_{CO_2,MEA} = k_{1,MEA}[CO_2][MEA] \text{ (primary amine)} \quad (6)$$

$$r_{CO_2,DEA} = k_{1,DEA}[CO_2][DEA] \text{ (primary amine)} \quad (7)$$

$$r_{CO_2,MDEA} = k_{1,MDEA}[CO_2][MDEA] \text{ (tertiary amine)} \quad (8)$$

and steric hindrance amine can be expressed as follows [14]:

$$r_{CO_2,AMP} = k_{1,AMP}[CO_2][AMP] \text{ (steric hindrance amine)} \quad (9)$$

The kinetics of piperazine [28] can be expressed as:

$$r_{CO_2,PZ} = k_{1,PZ}[CO_2][PZ] \quad (10)$$

For the case of $k_{-1}/(\sum(k_b[B]) \gg 1$, the reaction rate included the item $\sum k_B B/k_{-1}$. However, the overall reaction rate for the absorption of CO_2 into mixed amines can be expressed as:

$$r_{CO_2,OV} = r_{CO_2,MEA} + r_{CO_2,Add} \quad (11)$$

where, $r_{CO_2,Add}$ is the addition of a secondary amine, a tertiary amine, a steric hindrance amine, or piperazine into MEA solution.

In the absorption experiment, the packed column [29–31], the wetted wall absorber [10,14,32–34], the Rotating Packed Bed [4], the bubble column [11,35–38], and other

scrubbers [28,39] are often used. The operation of the packed column is complicated, and its operating costs are high, while the bubble column is characterized by its merits, as it has a controllable pH value, a high mass transfer coefficient, a high absorption factor, and it is easy to operate. Because of this, some researchers have adopted a bubble-column scrubber, as reported in the literature [11,35–38]. Therefore, the absorption experiment in this study is performed by using the bubble column with a mixed amine aqueous solution as the absorbent.

In this study, by using various mixed amines as solvents, a continuous bubble-column scrubber was adopted to study the effects of the type of mixed amines (A), the ratio of mixed amines (B), the liquid-flow rate (C), the gas-flow rate (D), and the concentration of total amines (E) on the removal efficiency (E_F), the absorption rate (R_A), the overall mass-transfer coefficients ($K_G a$), and the scrubbing factor (ϕ). This was because the E_F, the R_A, $K_G a$, and ϕ can be used to evaluate the performance of amines in the scrubbers and, hence, the best amines are selected. To reach the purpose, this could be accomplished effectively by using the Taguchi method [40], which is popularly known as the experimental design for industrial processes and covers many applications. For verification, the data reported here were used to evaluate the optimum data through the signal and noise (S/N) ratio analysis, which was used as a basis for the selection of mixed amines. Therefore, original research was carried out in this work. The schematic of the research is shown in Figure 1.

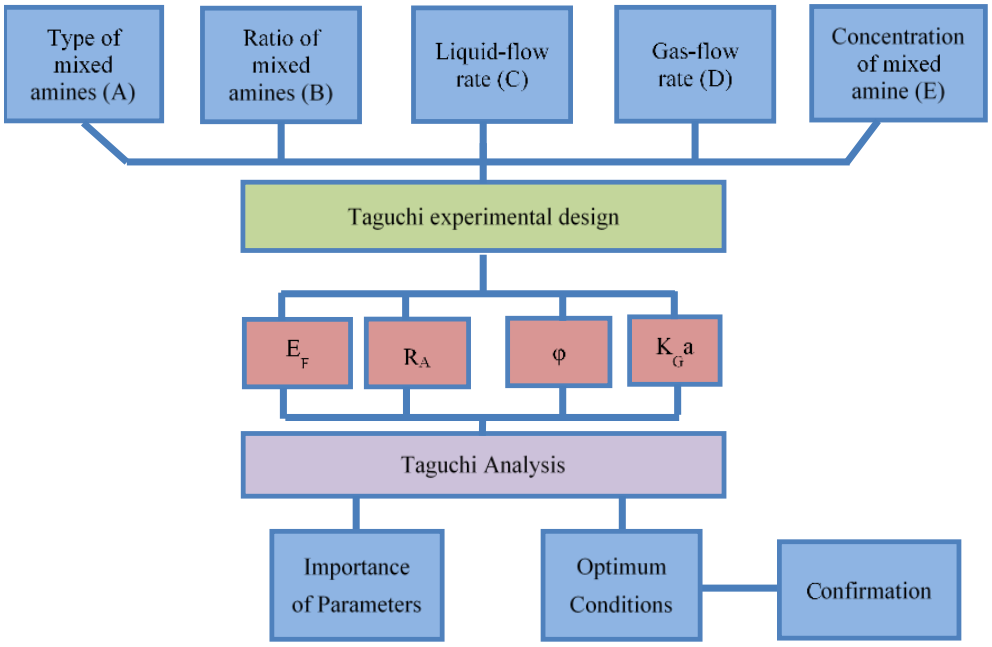

Figure 1. Framework of research conducted in this study.

2. Experimental Design and Procedure

2.1. Absorption Experiment Design

The aim of the experiment was to absorb CO_2 by using mixed amines in a bubble column. The results were expected to be applied to the absorption of CO_2 emitted by coal-fired power plants. Therefore, the CO_2 of flue gas in a coal-fired power plant at a 15% concentration of and at 50 °C was simulated to enter the column. According to previous works [41,42], the absorption of CO_2 in the bubble-column scrubber is affected by the gas flow rate, the liquid flow rate, the concentration of the solvent, as well as the temperature and pH. In order to select the mixed amines, the type of mixed amines (A), the ratio of mixed amines (B), the liquid-flow rate (C), the gas-flow rate (D), and the concentration of mixed amines (E) were considered as the condition factors, and four levels for each condition factor were taken respectively, i.e., the ratio of mixed amine (5–20 wt%), gas-flow rate, Q_g, (3–12 L/min), concentration of the mixed amines (1–2.5 M), and the liquid-flow rate, Q_L,

(0.15–0.3 L/min). Theoretically, a total of 1024 (=4^5) experiments needed to be conducted; however, to save time and experimental costs, we used the Taguchi experimental design to reduce the groups of the experiment to L_{16} (4^5) = 16. Here, the degree of freedom was found to be as follows [40]:

$$N = 1 + \sum_{i=1}^{NV} (L_i - 1) \quad (12)$$

where N is the degree of freedom, L_i is the level of the ith variable, and NV is the number of the variable. Using this equation, N = 1 + (3 + 3 + 3 + 3 + 3) is found to be 16, which is also the number of experiments. The value obtained in the steady-state for each experiment was adopted to obtain the absorption rate, the absorption efficiency, the scrubbing factor, and the overall volumetric mass transfer coefficient, and then the sequence of significance and optimum condition were obtained by using statistical software. Table 2 shows the conditions and levels, and Table 3 shows the orthogonal arrays. Finally, 16 groups of experiments needed to be conducted under different conditions.

Table 2. Factors and levels conducted in this study to examine the absorption and mass transfer phenomena of CO_2.

Factors	Level 1	Level 2	Level 3	Level 4
Type of mixed amines (A)	*MEA* + *AMP*	*MEA* + DIPA	*MEA* + TEA	*MEA* + *PZ*
Ratio of mixed amines [wt%] (B)	5	10	15	20
Q_L [mL/min] (C)	150	200	250	300
Q_g [L/min] (D)	3	6	9	12
Concentration of mixed amine [M] (E)	1	1.5	2	2.5

Table 3. The orthogonal arrays.

NO	A	B	C	D	E
1	1	1	1	1	1
2	1	2	2	2	2
3	1	3	3	3	3
4	1	4	4	4	4
5	2	1	2	3	4
6	2	2	1	4	3
7	2	3	4	1	2
8	2	4	3	2	1
9	3	1	3	4	2
10	3	2	4	3	1
11	3	3	1	2	4
12	3	4	2	1	3
13	4	1	4	2	3
14	4	2	3	1	4
15	4	3	2	4	1
16	4	4	1	3	2

The Taguchi method uses the signal and noise ratio (*S*/*N*) as the process optimization function [40,41]. The *S*/*N* value for larger-the-better is as follows:

$$\frac{S}{N} = -10 \times \log\left(\frac{1}{n}\sum_{1}^{n}\frac{1}{z_i^2}\right) \quad (13)$$

Here, n is the experimental number and z_i is the experimental data. Using this equation and experimental data, the optimum condition and parameter importance could be determined.

2.2. Calculation of Experimental Data

Experimental data, including the absorption efficiency, the absorption rate, the scrubbing factor, and the overall mass-transfer coefficient, were all evaluated in a steady-state condition. Based on the two-film model and materials balance, the absorption rate and overall volumetric mass-transfer coefficient could be derived [43]. The equations for this are as follows:

$$R_A = \frac{1}{V_L}\frac{Q_g P_{A1}}{RT}\left[1 - \left(\frac{1-y_{A1}}{y_{A1}}\right)\left(\frac{y_{A2}}{1-y_{A2}}\right)\right] \quad (14)$$

And

$$K_G a = \frac{Q_g}{V_L}\ln\left[\left(\frac{P_{A1}}{P_{A2}}\right)\left(\frac{T_2}{T_1}\right)\left(\frac{y_{A1}}{y_{A2}}\right)\right] \quad (15)$$

In Equation (15), it is assumed that the concentration of CO_2 gas in the liquid phase is extremely small and that it can be ignored ($C_A \gg HC_{AL}$) [43,44]. Therefore, the overall mass transfer coefficient can be derived. The result equation shows that $K_G a$ can be calculated from the known inlet and outlet conditions. In the above equations, y_A, V_L, Q_g, P_A, and T represent the mole fraction of CO_2, the final solution volume, the gas volumetric flow rate, the CO_2 gas partial-pressure, and the gas temperature, respectively. The notations of 1 and 2 represent the inlet and outlet, respectively.

In addition, the absorption efficiency and scrubbing factor [45] are shown as:

$$E_F = \frac{y_{A1} - y_{A2}}{y_{A1}} \times 100\% \quad (16)$$

And

$$\phi = \frac{F_A}{V_L F_L} \quad (17)$$

where F_A and F_L are the molar flow rate of CO_2-gas and the aqueous amine molar flow rate, respectively.

2.3. Experimental Devices and Procedures

The devices required for this experiment are shown in Figure 2 and include a bubble column, a gas-flow feed system (Bronkhorst, F-201CB DMFC), a liquid-flow system (Easy-Load, 7518-00), a pH-meter (Suntex, PC-310), a CO_2 m (Guardian Plus, D600), a gas heating system (5020 Data Acquisition System), and a liquid cooling system (Deng Yng, D-620). The range of a CO_2 m is 0–100%, while the confidence of a CO_2 m is $\pm 1 - 2\%$. In this experiment, the mixed amine was used as a test absorbent, which accounted for 5–20 wt % of the ratio in total amine concentration, which was in the range of 1–2.5 M. The required mixed amine concentration was prepared by using distilled water. Secondly, the flow rate of CO_2 and nitrogen input was based on the proportion of 15% of CO_2, and the gas inlet temperature was maintained at 50 °C. The experiment was started after the mixed amine was added to the column. During the experiment, the pH of the solution, the liquid temperature, the gas inlet temperature, the gas outlet temperature, the pressure, and the CO_2 concentration were recorded every five minutes. The liquid at the outlet was also withdrawn for titration to observe the concentration of carbonate in the scrubbed solution. At the end of the one-hour operation, the liquid input was closed and the solution was withdrawn by using a tubing pump to measure the volume of liquid (V_L) presented in the column.

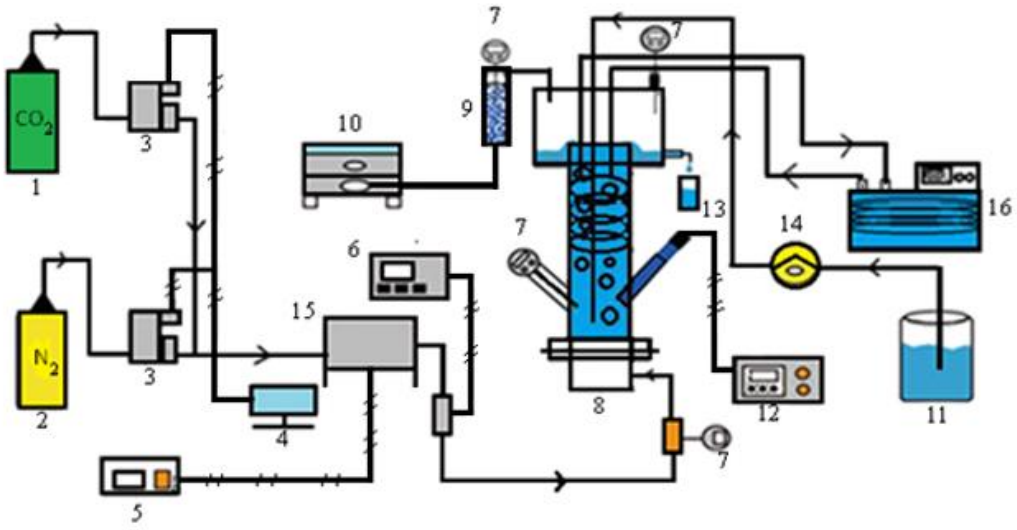

Figure 2. Experimental device for the absorption of CO_2.

3. Results and Discussion

3.1. Operation and Data Calculation of the Steady-State Condition

Using No. 1 as an example, the mixed amine was *MEA* + *AMP* (A), with the condition of 5% (B), 150 mL/min (C), 3 L/min (D), and 1 M (E). To understand the relationship of the outlet concentration of the gas, the gas temperature, the liquid temperature, the pH, and the inlet pressure against the duration of the operation, the measured value were divided by the initial value or setting value (such as the liquid temperature and gas inlet temperature) was defined as the Y (-) value, which was taken as the *y*-axis, and the time (t) was taken as the *x*-axis, as shown in Figure 3. After one hour, the Y-values were constant after 20 min, showing that the system had reached a steady state. Therefore, all data could be evaluated in a steady-state condition, i.e., after 20 min of operation. The CO_2 concentration dropped very low, indicating that the mixed amine had a high absorption efficiency. The analysis of the experimental results may be divided into two parts. Part 1 used the Taguchi method to design 16 groups of experiments that calculated the data, namely, the absorption rate, the absorption efficiency, the overall volumetric mass-transfer coefficient, and the scrubbing factor, as shown in Table 4. Part 2 searched for and confirmed the optimum condition and the sequence of significance, based on the results of the data that were calculated in Part 1 in the Taguchi analysis. Table 4 presents the values calculated by Equations (14)–(17), where the range of E is 61.33–100%, R_A is 4.02–26.48 $\times$ 10^{-4} (mol/s·L), K_Ga is 0.229–0.798 (s^{-1}), and ϕ is 0.034–0.263 (mole/mole·L). These data are comparable with those reported earlier [42,45,46]. Table 5 showed that the data obtained in this work, such as K_Ga in the range of 0.229–0.789 s^{-1}, were higher than that of the sodium glycinate solution (0.051–0.189 s^{-1}), the ammonia solution (0.0136–0.3302 s^{-1}), the NaOH solution (0.015–0.246 s^{-1}), and the *MEA* solution (0.0377–0.8881 s^{-1}). In addition, the R_A and E_F were also higher than the other systems listed in Table 5.

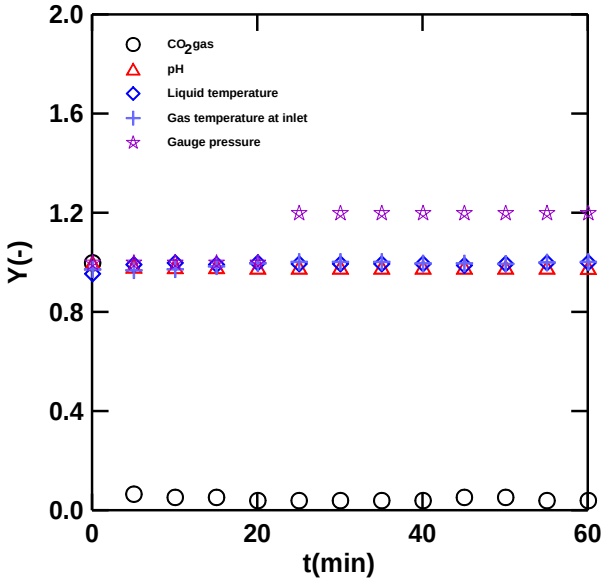

Figure 3. A plot of X vs. t, showing the steady-state operation (No.1).

Table 4. Experimental data obtained in this study.

NO.	E_F (%)	$R_A \times 10^4$ (mol/s·L)	$K_G a$ (s^{-1})	ϕ (mole/mole·L)
NO.1	95.95	4.02	0.229	0.134
NO.2	88.16	9.12	0.361	0.127
NO.3	84.00	14.47	0.523	0.106
NO.4	76.32	26.48	0.798	0.087
NO.5	85.33	14.40	0.536	0.108
NO.6	61.33	15.70	0.379	0.172
NO.7	96.05	4.21	0.235	0.046
NO.8	82.89	8.11	0.281	0.141
NO.9	68.42	27.7	0.730	0.154
NO.10	76.00	14.2	0.432	0.161
NO.11	92.00	8.54	0.394	0.104
NO.12	97.33	4.02	0.252	0.035
NO.13	89.33	8.13	0.340	0.126
NO.14	100	4.09	0.646	0.034
NO.15	62.67	15.6	0.382	0.263
NO.16	81.33	12.6	0.427	0.229

Table 5. Comparison of data obtained for different systems.

E_F (%)	$R_A \times 10^4$ (mol/s·L)	$K_G a$ (s^{-1})	System and Conditions	Reference
36.54–86.84	2.30–8.56	0.051–0.189	Sodium glycinate solution(pH-stat) pH = 9.5–11 Q_g = 3–9 L/min T = 25–40 °C C_L = 3–6 M y_{A1} = 15%	[42]
17.5–97.5	3.68–56.8	0.0377–0.8881	*MEA* solution(pH-stat) pH = 9–11 Q_g = 4–9.5 L/min T = 25–45 °C y_{A1} = 15–65%	[41]

Table 5. *Cont.*

E_F (%)	$R_A \times 10^4$ (mol/s·L)	$K_G a$ (s^{-1})	System and Conditions	Reference
10.9–100	3.21–10.99	0.0136–0.3302	Ammonia solution(pH-stat) pH = 9.5 Q_g = 4–9.5 L/min T = 25–60 °C y_{A1} = 15–60%	[45]
21.3–90.6	1.03–11.48	0.015–0.246	NaOH solution(pH stat) pH = 10–13 Q_g = 3–12 L/min T = 25–55 °C y_{A1} = 15%	[46]
61.33–100	4.02–27.70	0.229–0.789	Mixed amine solutions Q_g = 3–12 L/min Q = 150–300 mL/min T = 30 °C y_{A1} = 15%	This work

3.2. Taguchi Analysis

The values of the absorption efficiency (E_F), the absorption rate (R_A), the overall volumetric mass-transfer coefficient ($K_G a$), and the scrubbing factor (ϕ) were substituted into Equation (12) for a Taguchi *S/N* ratio analysis, and the results are shown in Figure 4 and Table 6. The parameters that significantly affected the E_F, R_A (or ϕ), and $K_G a$ were in the order of D > E > A > B > C, D > E > C > B > A, and D > E > C > A > B, respectively. The importance of each parameter can be quantified and can be expressed in a radar chart, as shown in Figure 5. The scope was in the range 1 to 5, such as the importance of parameters in E_F, (D(5) > E(4) > A(3) > B(2) > C(1)), which are shown in the form of dotted lines. While R_A (A1B3C4D4E2) and ϕ (A1B1C1D4E1) appeared to have the same radar chart, they had different optimum conditions. The data showed that D (the gas-flow rate), and E (the concentration of mixed amine) were the primary factors, while A (the type of mixed amines), and B (the percentage of mixed amines) were the minor factors. The optimum conditions for E_F and $K_G a$ were A1B4C4D1E4 and A4B2C3E4D4, respectively. It also revealed the type of mixed amine (A1, *MEA + AMP*) that was dominant for E_F, R_A, and ϕ, and the type of mixed amine (A4, *MEA + PZ*) that was better for $K_G a$. However, the optimum conditions still need to be confirmed.

Table 6. Optimum conditions and importance of parameters.

Outcome Data	Optimum Conditions	Importance of Parameters
E_F	A1 B4 C4 D1 E4	D > E > A > B > C
R_A	A1 B3 C4 D4 E2	D > E > C > B > A
$K_G a$	A4 B2 C3 D4 E4	D > E > C > A > B
ϕ	A1 B1 C1 D4 E1	D > E > C > B > A

3.3. Confirmation of the Optimum Condition

Four experiments were carried out, based on the optimum conditions, and the results are presented in Table 7. The values obtained were 100%, 30.69 mol/s·L, 1.54 s^{-1}, and 0.297 mol/mol·L for E_F, R_A, $K_G a$, and ϕ, respectively. These are the largest values, and the larger-the-better, indicating that the optimum conditions could be confirmed here. This also demonstrated that the Taguchi method that was used was efficient.

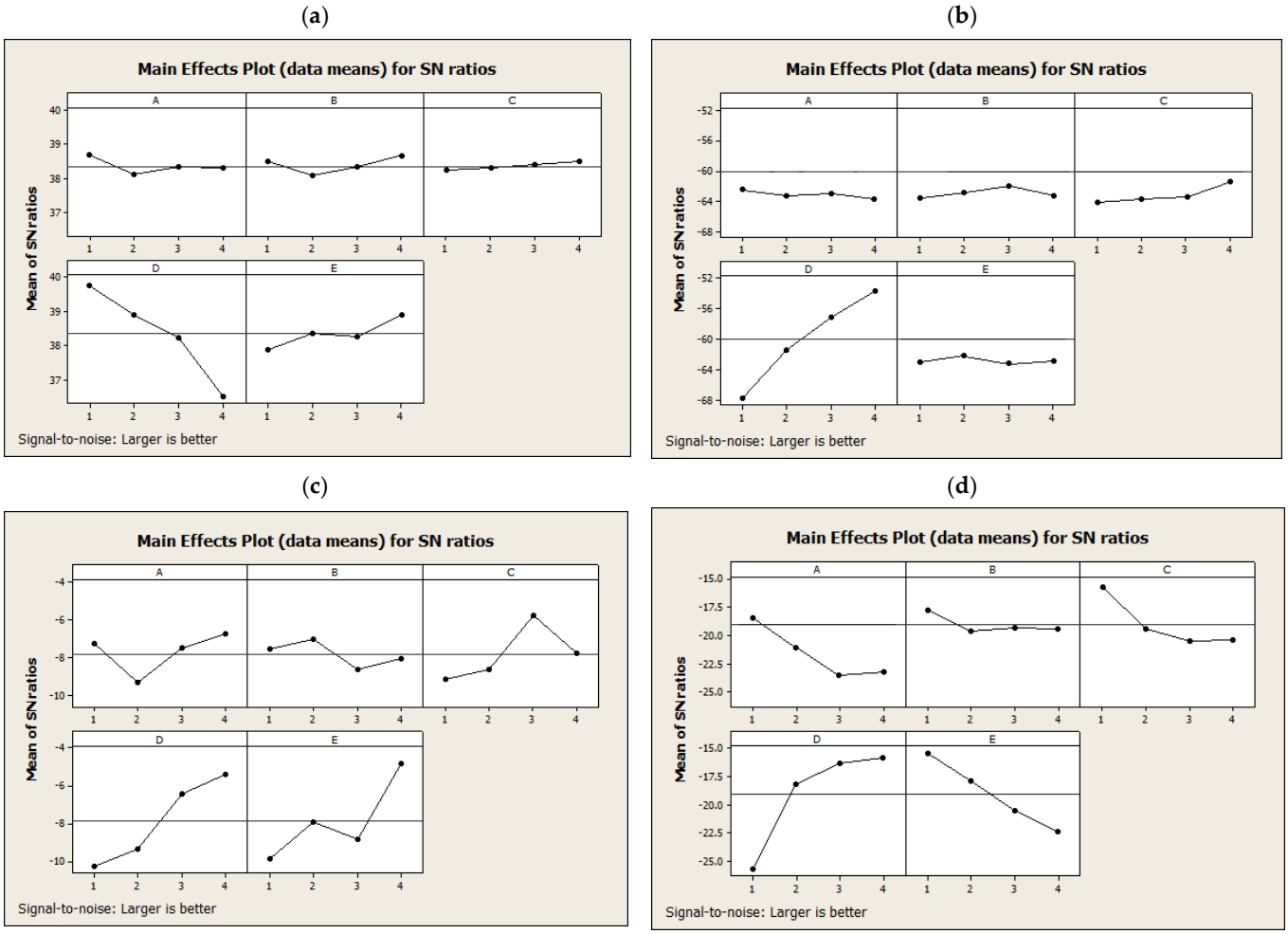

Figure 4. The larger-the-better for various outcome data are obtained from Taguchi analysis. (**a**) E_F; (**b**) R_A; (**c**) K_Ga; (**d**) ϕ.

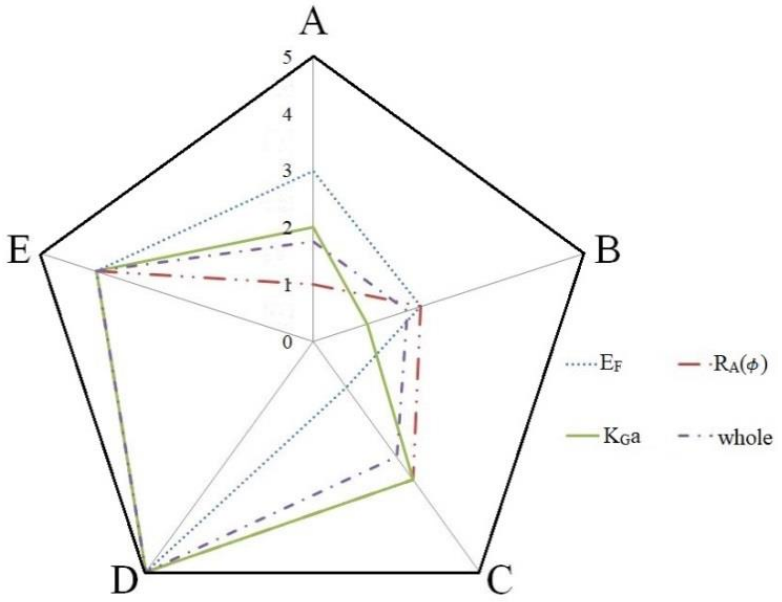

Figure 5. A radar chart showing the importance of the parameters.

Table 7. Confirmation of the optimum condition.

NO.	E_F (%)	$R_A \times 10^4$ (mole/s·L)	$K_G a$ (s^{-1})	ϕ (mole/mole·L)
1–16	61.33–100	4.02–27.7	0.229–0.798	0.034–0.263
Optimum value	100	30.69	1.540	0.297

3.4. Comparisons of Mixed Amines

To compare the outcome data obtained in Table 4, the bar graphs were plotted for E_F, R_A, $K_G a$, and ϕ, respectively, as shown in Figure 6. From the bar charts, the mixed amine *MEA* + *AMP* appears to be better, compared to the others, except for ϕ. In order to obtain a quantitative comparison, the average value of each group, i.e., *AMP*, DIPA, TEA, and *PZ*, was required. Using E_F as an example, the average values for *AMP*, DIPA, TEA, and *PZ* were 86.1, 81.4, 83.4, and 83.3, respectively. The sequence of the value was expressed as excellent (◎), good (○), fair (△), and poor (×), respectively. The R_A, $K_G a$, and ϕ can also be estimated by using the same method. The results of the estimation of each item are listed in Table 8. Cumulatively, the significant sequence of mixed amine was A1(*MEA* + *AMP*) > A3(*MEA* + TEA) > A4(*MEA* + *PZ*) > A2 (*MEA* + DIPA). This shows that the mixed amine (*MEA* + *AMP*) was the best.

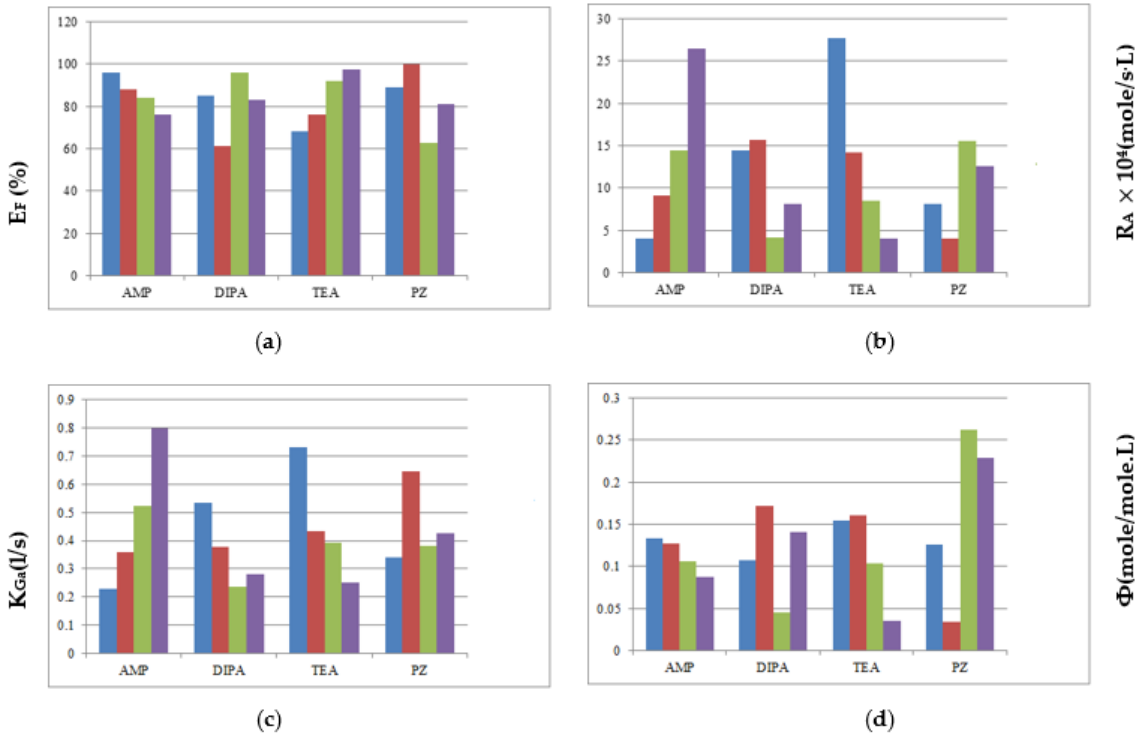

Figure 6. Bar charts of mixed amine for the comparison of various outcome data (respectively, NO.1 to NO.16). (**a**) Absorption efficiency; (**b**) Absorption rate; (**c**) Overall mass transfer coefficient; (**d**) Scrubbing factor.

Table 8. Comparison of mixed amines in the outcome data.

Mixed Amines	*AMP*	DIPA	TEA	*PZ*
E_F	◎	×	○	△
R_A	○	△	◎	×
$K_G a$	◎	×	○	△
ϕ	△	○	△	◎

The sequence of the value was expressed as excellent (◎), good (○), fair (△), and poor (×), respectively.

4. Conclusions

A continuous bubble-column scrubber was used successfully to select mixed amines in the CO_2 capture process, by using the absorption efficiency (E_F), the absorption rate (R_A), the overall mass transfer coefficient (K_Ga), and the scrubbing factor (ϕ) as indicators. A total of 16 runs were carried out, using Taguchi's experimental design, which greatly reduced the number of experiments required. According to the Taguchi analysis, the mixed amine (*MEA* + *AMP*) had a better E_F, R_A, and ϕ, while the mixed amine (*MEA* + *PZ*) had a better K_Ga. The major factors affecting the outcome data were found to be the gas-flow rate (D) and the concentration of mixed amines (E). A confirmation of the optimum conditions showed that the most optimum values of E_F (100%), R_A (30.69 × 10^{-3} mol/s·L), K_Ga (1.540 s^{-1}), and ϕ (0.297), fitted into the larger-the-better category. From the radar chart and bar chart analyses, the significant sequence of mixed amines was found to be A1 (*MEA* + *AMP*) > A3 (*MEA* + TEA) > A4 (*MEA* + *PZ*) > A2 (*MEA* + DIPA). This result indicated that the mixed amine (*MEA* + *AMP*) performed the best in the CO_2 capture process under the operating conditions of this study. In this case, A1B4C4D4E4 is the best for K_Ga and R_A, while A1B1C1D1E1 is the best for E_F and ϕ. In future, mixed amine (*MEA* + *AMP*) can be improved further by adding TEA, to improve the $R_{A,}$ and the addition of *PZ*, to improve ϕ.

Author Contributions: Conceptualization, P.-C.C. and H.-H.C.; methodology, P.-C.C.; data curation, P.-C.C., H.-H.C., J.-H.J. and C.-H.K.; resources, P.-C.C., H.-H.C., J.-H.J. and C.-H.K.; writing—original draft preparation, P.-C.C., H.-H.C., J.-H.J. and C.-H.K.; writing—review and editing, P.-C.C. and H.-H.C.; funding acquisition, P.-C.C. All authors have read and agreed to the published version of the manuscript.

Funding: This work was supported by the MOST in Taiwan.

Institutional Review Board Statement: The study was conducted according to the guidelines of the Declaration of Helsinki, and approved by the Institutional Review Board (or Ethics Committee) of Lunghwa University of Science and Technology.

Informed Consent Statement: Informed consent was obtained from all subjects involved in the study.

Data Availability Statement: Please refer to special production in Dept. of Chemical and Materials Engineering, Lunghwa University of Science and Technology.

Acknowledgments: The authors acknowledge the financial supports of the MOST in Taiwan (MOST-109-2221-E-262-004) and the Research Institute of Taiwan Power Company.

Conflicts of Interest: The authors declare no conflict of interest. The founding sponsors had no role in the design of the study; collection, analyses, or interpretation of the data; writing of the manuscript; or the decision to publish the results.

References

1. Ho, M.T.; Allinson, G.W.; Wiley, D.E. Comparison of *MEA* capture cost for low CO2 emissions sources in Australia. *Int. J. Greenh. Gas Con.* **2011**, *5*, 49–60. [CrossRef]
2. Han, K.; Ahn, C.K.; Lee, M.S. Performance of an ammonia-based CO2 Capture pilot facility in iron and steel industry. *Int. J. Greenh. Gas Con.* **2014**, *27*, 239–246. [CrossRef]
3. Li, T.; Keener, T.C. A review: Desorption of CO2 from rich solutions in chemical absorption processes. *Int. J. Greenh. Gas Con.* **2016**, *51*, 290–304. [CrossRef]
4. Yu, C.H.; Huang, C.H.; Tan, C.S. A Review of CO2 Capture by Absorption and Adsorption. *Aerosol. Air Qual. Res.* **2012**, *12*, 745–769. [CrossRef]
5. Abdulkadir, A.; Rayer, A.V.; Quang, D.V.; Hadri, N.E.; Dindi, A.; Feron, P.H.M.; Abu-Zahra, M.R.M. Heat of absorption and specific heat of carbon dioxide in aqueous solutions of monoethanolamine, 3-piperdienmethonal and their blends. *Energy Procedia* **2014**, *63*, 2070–2081. [CrossRef]
6. Vaidya, P.D.; Kenig, E.Y. Absorption of CO2 into aqueous blends of alkanolamines prepared from renewable resources. *Chem. Eng. Sci.* **2007**, *62*, 7344–7350. [CrossRef]
7. Zhang, X.; Zhang, C.F.; Qin, S.J.; Zheng, Z.S. A kinetics study on the absorption of carbon dioxide into mixed aqueous solution of methyldiethanolamine and piperazine. *Ind. Eng. Chem. Res.* **2001**, *40*, 3785–3791. [CrossRef]
8. Van Wagener, D.H.; Rochelle, G.T. Stripper configurations for CO2 capture by aqueous monoethanolamine and piperazine. *Energy Procedia* **2011**, *4*, 1323–1330. [CrossRef]

9. Adeosun, A.; Abu-Zahra, M.R.M. Evaluation of amine-blend solvent systems for CO_2 post-combustion capture applications. *Energy Procedia* **2013**, *37*, 211–218. [CrossRef]
10. Ali Khan, A.; Halder, G.; Saha, A.K. Kinetic effect and absorption performance of piperizine activator into aqueous solutions of 2-amino-1-methyl-1-propanol through post-combustion CO_2 capture. *Korean J. Chem. Eng. Eng.* **2019**, *63*, 1090–1101. [CrossRef]
11. Mondal, M.K. Absorption of carbon dioxide into a mixed aqueous solution of diethanolamine and piperazine. *Indian J. Chem. Technol.* **2010**, *17*, 431–435.
12. Vaidya, P.D.; Kenig, E.Y. CO_2-alkanomine reaction kinetics: A review of recent work. *Chem. Eng. Technol.* **2007**, *30*, 1467–1474. [CrossRef]
13. Rangwala, H.A.; Morrell, B.R.; Mather, A.E.; Otto, F.D. Absorption of CO_2 into aqueous tertiary amine/mea solutions. *Can. J. Chem. Eng.* **1992**, *70*, 482–490. [CrossRef]
14. Xiao, J.; Li, C.C.; Li, M.H. Kinetics of absorption of carbon dioxide into aqueous solutions of 2-amino-2-methyl-1-propanol+monoethanolamine. *Chem. Eng. Sci.* **2000**, *55*, 161–175. [CrossRef]
15. Choi, W.J.; Seo, J.B.; Jang, S.Y.; Jung, J.H.; Oh, K.J. Removal characteristics of CO2 using aqueous *MEA/AMP* solutions in the absorption and regeneration process. *J. Environ. Sci.* **2009**, *21*, 907–913. [CrossRef]
16. Neveux, T.; Moullec, Y.L.; Corriou, J.P.; Favre, E. Energy performance of CO_2 capture processes: Interaction between process design and solvent. *Chem. Eng. Trans.* **2013**, *35*, 337–342. [CrossRef]
17. Dash, S.K.; Samanta, A.N.; Bandyopadhyay, S.S. Simulation and parametric study of post combustion CO_2 capture process using (*AMP+PZ*) blended solvent. *Inter. J. Greenh. Gas. Con.* **2014**, *21*, 130–139. [CrossRef]
18. Diao, Y.F.; Zheng, X.Y.; He, B.S.; Chen, C.H.; Xu, X.C. Experimental study on capuring CO2 greenhouse gas by ammonia scrubbing. *Energy Convers. Manag.* **2004**, *45*, 2283–2296. [CrossRef]
19. Oyenekan, B.A.; Rochelle, G.T. Alternative stripper configurations for CO_2 capture by aqueous amines. *AICHE J.* **2007**, *53*, 3144–3154. [CrossRef]
20. Daneshvar, N.; Moattar, M.T.Z.; Abdi, M.A.; Aber, S. Carbon dioxide equilibrium absorption in muti-component systems of CO2+TIPA+*MEA*+H2O, at low CO2 partial pressures: Experimental solubility data, corrosion study and molding with artificial neural network. *Sep. Purif. Technol.* **2004**, *37*, 135–147. [CrossRef]
21. Mangalapally, H.P.; Notz, R.; Hoch, S.; Asprion, N.; Sieder, G.; Garcia, H.; Hasse, H. Pilot plant Experimental studies of post combustion CO_2 capture by reactive absorption with *MEA* and new solvents. *Energy Procedia* **2009**, *1*, 963–970. [CrossRef]
22. Kim, J.H.; Lee, J.H.; Lee, I.Y.; Jang, K.R.; Shim, J.G. Performance evaluation of newly developed absorbents for CO_2 capture. *Energy Procedia* **2011**, *4*, 81–84. [CrossRef]
23. Wen, J.Q.; Liu, D.W.; Kirk, D.W.; Yang, J.; Bao, S. Aqueous blended amine *MEA*+DETA solutions for CO_2 absorption. *APEST* **2012**, *6*, 459–464.
24. Lin, P.H.; Wong, D.S.H. Carbon dioxide capture and regeneration with amine/alchol/water. *Int. J. Greenh. Gas Con.* **2014**, *26*, 69–75. [CrossRef]
25. Bosch, H.; Versteeg, G.F.; van Swaaij, W.P.M. Gas-liquid mass transfer with parallel reversible reactions—III. Absorption of CO_2 into solutions of blends of amines. *Chem. Eng. Sci.* **1989**, *44*, 2745–2750. [CrossRef]
26. David, A.; James, G.; Critchfield, E.; Rochelle, G.T. CO_2 absorption/desorption in mixtures of methyldiethanolamine with monoethanolamine. *Chem. Eng. Sci.* **1991**, *46*, 2829–2845. [CrossRef]
27. Versteeg, G.F.; Dijck, L.A.J.; Swaaij, W.P.M. On the kinetics between CO_2 and Alkaloamines both in aqueous and non-aqueous solutions. An overview. *Chem. Eng. Commun.* **1996**, *114*, 113. [CrossRef]
28. Derks, P.W.J.; Kleigeld, T.; van Aken, C.; Hogendoorn, J.A.; Versteeg, G.F. Kinetics of absorption of carbon dioxide in aqueous piperazine solutions. *Chem. Eng. Sci.* **2006**, *61*, 6837–6854. [CrossRef]
29. Aroonwilas, A.; Veawab, A. Integration of CO_2 capture unit using blended *MEA-AMP* solution into coal-fired power plants. *Energy Procedia* **2009**, *1*, 4315–4321. [CrossRef]
30. Badea, A.A.; Dinca, C.F. CO_2 capture from post-combustion gas by employing *MEA* absorption process–experimental investigation for pilot studies. *UPB Sci. Bull. Ser. D* **2012**, *74*, 21–32.
31. Fu, K.; Chen, G.; Sema, T.; Zhang, X.; Liang, Z. Experimental study on mass transfer and prediction using artificial neural network for CO_2 absorption into aqueous DETA. *Chem. Eng. Sci.* **2013**, *100*, 195–202. [CrossRef]
32. Bishnoi, S.; Rochelle, G.T. Absorption of carbon dioxide into aqueous piperazine: Reaction kinetics, mass transfer and solubility. *Chem. Eng. Sci.* **2000**, *55*, 5531–5543. [CrossRef]
33. Sakwattanapong, R.; Aroonwilas, A.; Veawab, A. Reaction rate of CO2 in aqueous *MEA-AMP* solution: Experiment and modeling. *Energy Procedia* **2009**, *1*, 217–224. [CrossRef]
34. Rodriguez, H.; Mello, L.; Salvagnini, W.; de Paulo, J.L. Absorption of carbon dioxide into aqueous solutions of alkanolamines in wetted wall column with film promoter. *Chem. Eng. Trans.* **2011**, *25*, 51–56. [CrossRef]
35. Gómez-Díaz, D.; López, A.B.; La García, M.D.R.; Pacheco, R.R.; Gómez-Díaz, D. Carbon Dioxide Absorption in Triethanolamine Aqueous Solutions: Hydrodynamics and Mass Transfer. *Chem. Eng. Technol.* **2014**, *37*, 419–426. [CrossRef]
36. Al-Hindi, M.; Azizi, F. The effect of water type on the absorption and desorption of carbon dioxide in bubble columns. *Chem. Eng. Comm.* **2020**, *207*, 339–349. [CrossRef]
37. Karamian, S.; Mowla, D. Esmaeilzadeh, The effect of various nanofluids on absorption intensification of CO_2/SO_2 in a single-bubble column. *Processes* **2019**, *7*, 393. [CrossRef]

38. Beiki, H.; Ansaryan, O. Nanofluids application to promote CO_2 absorption inside a bubble column: ANFIS and experimental study. *Energy* **2020**, unpublished.
39. Chakma, A.; Lemonier, J.P.; Chornet, E.; Overend, R.P. Absorption of CO2by aqueous triethanolamine (TEA) solutions in a high shear jet absorber. *Gas Sep. Purif.* **1989**, *3*, 65–70. [CrossRef]
40. Fraley, S.; Oom, M.; Terrien, B.; Zalewski, J. Design of Experiments via Taguchi Methods: Orthogonal Arrays. 2012. Available online: https://controls.engin.umich.edu/wiki/index.php (accessed on 13 January 2021).
41. Chen, P.C.; Luo, Y.X.; Cai, P.W. CO_2 Capture Using Monoethanolamine in a Bubble-ColumnScrubber. *Chem. Eng. Technol.* **2015**, *38*, 274–282. [CrossRef]
42. Chen, P.C.; Lin, S.Z. Optimization in the Absorption and Desorption of CO_2 Using Sodium Glycinate Solution. *Appl. Sci.* **2018**, *8*, 2041. [CrossRef]
43. Chen, P.C.; Shi, W.; Du, R.; Chen, V. Scrubbing of CO2 Greenhouse gases, accompanied by precipitation in a continuous bubble-column Scrubber. *Ind. Eng. Chem. Res.* **2008**, *47*, 6336–6343. [CrossRef]
44. Jou, F.Y.; Mather, A.E.; Otto, F.D. The solubility of CO_2 in a 30 mass percent monoethanolamine solution. *Can. J. Chem. Eng.* **1995**, *73*, 140–147. [CrossRef]
45. Chen, P.C.; Yu, S.C. CO_2 Capture and Crystallization of Ammonia Bicarbonate in a Lab-Scale Scrubber. *Crystals* **2018**, *8*, 39. [CrossRef]
46. Chen, P.C.; Huang, C.H.; Su, T.; Chen, H.W.; Yang, M.W.; Tsao, J.M. Optimum conditions for thecapture of carbon dioxide with a bubble-column scrubber. *Int. J. Greenh. Gas Con.* **2015**, *35*, 47–55. [CrossRef]